



1,3-Dialkyl-8-(hetero)aryl-9-OH-9-deazaxanthines as potent A_{2B} adenosine receptor antagonists: Design, synthesis, structure–affinity and structure–selectivity relationships

Angela Stefanachi^a, Orazio Nicolotti^a, Francesco Leonetti^a, Saverio Cellamare^a, Francesco Campagna^a, Maria Isabel Loza^b, Jose Manuel Brea^b, Fernando Mazza^c, Enrico Gavuzzo^{d,*}, Angelo Carotti^{a,*}

^a Dipartimento Farmaco-chimico, Università degli Studi di Bari, via Orabona 4, I-70125 Bari, Italy

^b Departamento de Farmacologia, Universidade de Santiago de Compostela, E-15782 Santiago de Compostela, Spain

^c Dipartimento di Chimica, Ingegneria Chimica e dei Materiali, Università dell'Aquila, I-67100 L'Aquila, Italy

^d CNR, Montelibretti, I-00016 Monterotondo Scalo (Rome), Italy

ARTICLE INFO

Article history:

Received 17 July 2008

Revised 19 September 2008

Accepted 26 September 2008

Available online 30 September 2008

Keywords:

1,3-Dialkyl-8-(hetero)aryl-9-OH-9-deazaxanthines

Adenosine receptor antagonists

Structure–affinity relationships

Structure–selectivity relationships

X-ray crystallography

ABSTRACT

A number of 1,3-dialkyl-8-(hetero)aryl-9-OH-9-deazaxanthines were prepared and evaluated as ligands of recombinant human adenosine receptors ($hARs$). Several 1,3-dipropyl derivatives endowed with nanomolar binding affinity at hA_{2B} receptors, but poor selectivity over hA_{2A} , hA_1 and hA_3 AR subtypes were identified. A comparison with the corresponding 7-OH- and 7,9-unsubstituted-deazaxanthines revealed that 9-OH-9-deazaxanthines are more potent hA_{2B} ligands with lower partition coefficients and higher water solubility compared to the other two congeneric classes of deazaxanthines. An optimization of the *para*-substituent of the 8-phenyl ring of 9-OH-9-deazaxanthines led to the discovery of compound **38**, which exhibited outstanding hA_{2B} affinity ($K_i = 1.0$ nM), good selectivity over hA_{2A} , hA_1 and hA_3 (selectivity indices = 100, 79 and 1290, respectively) and excellent antagonist potency in a functional assay on rat A_{2B} ($pA_{2B} = 9.33$).

© 2008 Published by Elsevier Ltd.

1. Introduction

Adenosine is an endogenous purine nucleoside that modulates several important physiological processes^{1–3} by triggering four diverse G-protein-coupled adenosine receptors (ARs), named A_1 , A_{2A} , A_{2B} and A_3 .⁴ ARs differ in amino acid sequence, tissue distribution, effector coupling, and biological and pharmacological profiles. Among AR ligands, A_{2B} selective receptor antagonists have recently been the object of intense medicinal chemistry research since growing evidence has indicated a variety of potential therapeutic applications^{5–16} at the gastrointestinal (e.g., diarrhea)⁷ and neurological levels (e.g., Alzheimer's disease and dementia),⁸ in hypersensitive disorders (e.g., asthma),^{12–16} diabetes,⁹ atherosclerosis,¹⁷ restenosis,¹⁸ and cancer.¹¹ In this challenging scenario we focused our attention on the discovery of selective A_{2B} antagonists as potential antiasthmatic agents. The rationale of this investigation stems from the observation that the bronchodilating activity of two xanthinic drugs, that is, theophylline and enprofylline, might be due to selective, albeit small, antagonism at the A_{2B} AR.¹⁹ These findings prompted

several groups to design and test a large number of xanthine derivatives in search for new, more potent and A_{2B} -selective ligands.^{20–23} Indeed, in the last few years very potent and highly A_{2B} -selective xanthines have been discovered.^{24–28} Some of them, namely XAC (**1**),²⁹ MRS1754 (**2**),³⁰ **3**,³⁰ **6**,³¹ **7**,³² and **8**,^{33,34} are reported in Chart 1.

Within this line of research, we recently reported the design, synthesis, and structure–activity (SAR) and structure–selectivity relationship (SSR) studies of a large series of 9-deazaxanthines (9-dAXs), a less exploited class of AR ligands, leading to the discovery of very potent and selective A_{2B} antagonists (e.g., **4** and **5** in Chart 1).^{35,36}

A direct comparison of the molecular electrostatic potentials (MEPs) of xanthine and 9-dAX model compounds indicated in the latter the lack of the deepest MEP minimum observed near N-9 in xanthines.³⁷ As a consequence, the ability of 9-dAXs to form hydrogen bonds (HBs) and/or participate in other electrostatic (polar) interactions was strongly diminished. In fact, despite their excellent affinity and selectivity profiles, 9-dAXs displayed lower water solubility, higher partition coefficients and poorer pharmacokinetic properties compared to xanthines which hampered their preclinical development as antiasthmatic drugs.²⁵ To improve the pharmacokinetic properties of 9-dAXs, it was deemed necessary to design new and more polar analogues, possibly through an easily accessible synthetic pathway.

* Corresponding author. Tel.: +39 080 5442782; fax: +39 080 5442230.

E-mail address: carotti@farmchim.uniba.it (A. Carotti).

* Deceased.

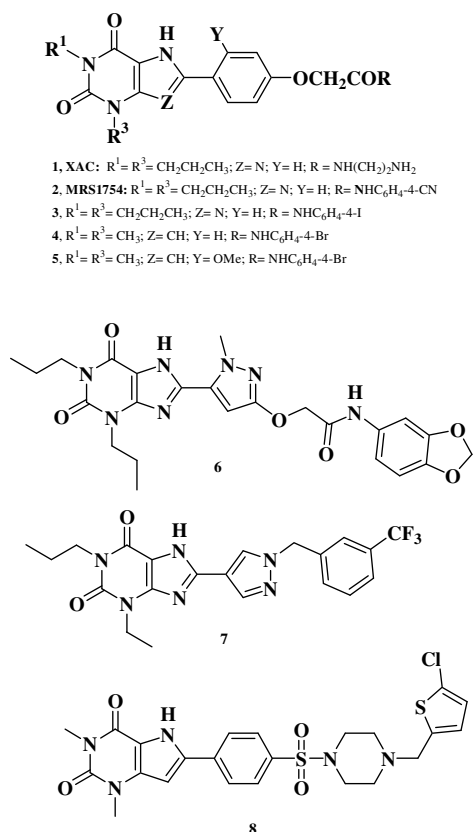


Chart 1. Xanthine and 9-dAX derivatives with potent A_{2B} AR antagonistic activities (**1–8**).

Serendipitously, we found a simple, viable and efficient solution to our problem.

While performing the first reaction of a two-step synthetic pathway, outlined in Scheme 1,³⁸ to prepare the 1,3-dipropyl-8-*p*-nitrophenyl-9-dAX, instead of the styryl derivative **III**, unexpectedly, a compound with a molecular weight of a hydroxy-9-dAX was obtained as a unique reaction product.

Even if a careful examination of the analytical and spectral data suggested a 9-OH-9-dAX derivative as the most likely chemical structure, an unequivocal and definitive structural assignment was required because, to the best of our knowledge, 9-OH-9-dAXs had never been produced under such relatively mild experimental conditions (Scheme 2). A literature search indicated that 9-OH-9-dAXs had already been reported by Senda et al.³⁹ as by-products of the photoreductive cyclization of 5-nitro-6-styryl-uracil, and by

Yoneda et al.^{40,41} under more severe experimental conditions (in refluxing DMF for a few hours). Therefore, we decided to carry out an X-ray diffractometric study to unequivocally assign the 9-OH-9-dAX structure to the isolated compound **32** (Table 1). Figure 1 shows a stereo view of the X-ray crystallographic structure of **32** that was identified as a 9-OH-9-dAX derivative. The dihedral angle between the mean planes of the 9-dAX and the 8-phenyl rings was nearly 25° . This conformation was a compromise between electron delocalization on the entire π system and steric hindrance among facing non-bonded atoms of the two close ring systems. Both propyl chains were in trans conformation and protruded out of the plane of the heterocyclic system on the same side. The 9-hydroxyl hydrogen laid outside the pyrrole ring plane but on the opposite side of the propyl chains.

Once the correct chemical structure to our compound was assigned, we decided to apply the synthetic approach illustrated in Scheme 2 to prepare a properly designed series of 1,3-dialkyl-9-OH-8(hetero)aryl-9-dAXs aiming at the discovery of new, highly potent and selective A_{2B} antagonists with improved pharmacokinetic properties compared to the corresponding isomeric 7-OH- and 7,9-unsubstituted-9-dAXs. During the execution of our work, a patent reporting one 1,3-dipropyl-9-OH-9dAX, that is, the 8-(*p*-CN-phenyl) derivative, along with a series of other heterocyclic AR antagonists to treat ischemia reperfusion injury, was filed to Biogen. Inc.⁴²

A preliminary comparative modeling study was performed on two reference molecules, that is, 9-dAX derivative **A** and 9-OH-9-dAX derivative **B** (depicted in Chart 2), to analyze how the different electronic distributions, HB-making ability and hydrophobic properties of the two classes of molecules would have resulted in improved pharmacokinetic properties.

2. Chemistry

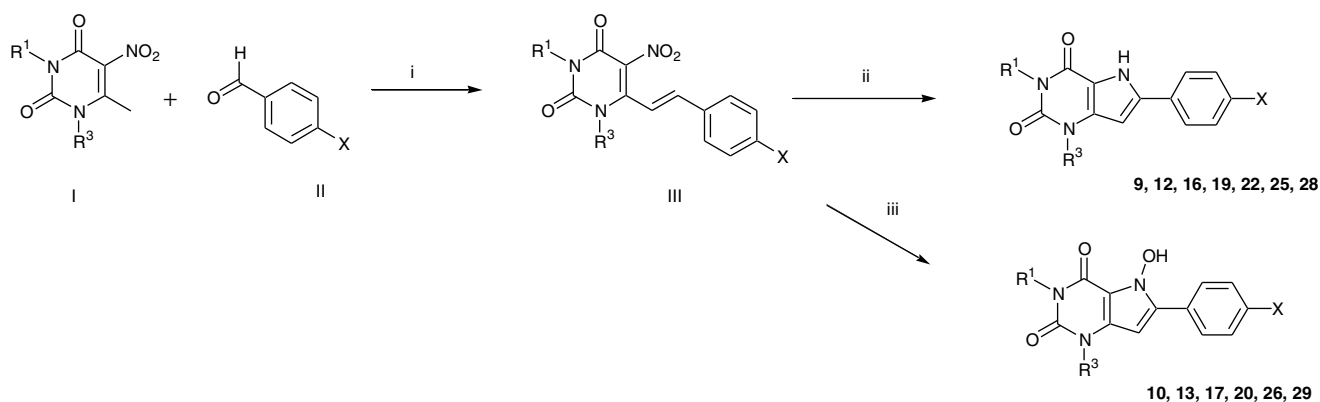
The synthesis of 8-substituted-9-OH-9-dAXs was first successfully improved by applying microwave heating to the reaction illustrated below in Scheme 3.

9-OH-9-dAXs were obtained in medium-to-high yields, in a very short time-frame (15 min), in DMF at 200°C by microwave irradiation at a maximum power of 400 W.

8-Anilino derivative **24** was obtained by a SnCl_2 -mediated reduction of the corresponding nitroderivative **32** whereas 8-anilino derivative **23** was synthesized by basic hydrolysis of 7-OH-8-(4-acetamidophenyl)-9-dAX intermediate.³⁷

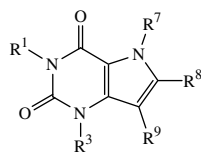
8-(*p*-OH-phenyl)-9-OH-9-dAX **27** was prepared by demethylation of methoxy derivative **30** with BBR_3 .

8-Substituted-7-OH-9-dAXs **10** and **26**, and the novel 9-dAX **25**, were obtained from 1,3-dialkyl-5-nitro-6-styryl uracil by a reductive cyclization with SnCl_2 in DMF at room temperature or under reflux, respectively, according to our reported method.³⁸



Scheme 1. Reagents and conditions: (i) Piperidine, EtOH reflux; (ii) SnCl_2 , DMF, reflux; (iii) SnCl_2 , DMF, r.t.

Table 1
Chemical structures and AR binding affinities^a of 1,3-dialkyl-8-(hetero)aryl-9-dAX derivatives **9–37**



Compounds	R ¹	R ³	R ⁷	R ⁹	R ⁸	K _i hA _{2B}	K _i hA _{2A}	SI ^b	K _i hA ₁ ^c	K _i hA ₃ ^c
9	CH ₃	CH ₃	H	H	C ₆ H ₅	182	479	2.6	nd	nd
10	CH ₃	CH ₃	OH	H	C ₆ H ₅	1660	12%	nd	nd	nd
11	CH ₃	CH ₃	H	OH	C ₆ H ₅	288	1470	5.1	nd	nd
12	CH ₃	CH ₃	H	H	4-CH ₃ -C ₆ H ₄	457	126	0.28	nd	nd
13	CH ₃	CH ₃	OH	H	4-CH ₃ -C ₆ H ₄	2239	8%	nd	nd	nd
14	CH ₃	CH ₃	H	OH	4-CH ₃ -C ₆ H ₄	513	2450	4.8	nd	nd
15	CH ₃	CH ₃	H	OH	4-CH ₃ SO ₂ -C ₆ H ₄	68	692	10.2	nd	nd
16	nC ₃ H ₇	nC ₃ H ₇	H	H	C ₆ H ₅	229	646	2.8	34	96
17	nC ₃ H ₇	nC ₃ H ₇	OH	H	C ₆ H ₅	676	32%	nd	25	30%
18	nC ₃ H ₇	nC ₃ H ₇	H	OH	C ₆ H ₅	54	50	0.93	83	182
19	nC ₃ H ₇	nC ₃ H ₇	H	H	4-CH ₃ -C ₆ H ₄	199	631	3.2	nd	nd
20	nC ₃ H ₇	nC ₃ H ₇	OH	H	4-CH ₃ -C ₆ H ₄	589	398	0.66	nd	nd
21	nC ₃ H ₇	nC ₃ H ₇	H	OH	4-CH ₃ -C ₆ H ₄	89	89	1	nd	nd
22	nC ₃ H ₇	nC ₃ H ₇	H	H	4-NH ₂ -C ₆ H ₄	8.9	162	18.2	nd	nd
23	nC ₃ H ₇	nC ₃ H ₇	OH	H	4-NH ₂ -C ₆ H ₄	155	240	1.5	nd	nd
24	nC ₃ H ₇	nC ₃ H ₇	H	OH	4-NH ₂ -C ₆ H ₄	19	166	8.7	nd	nd
25	nC ₃ H ₇	nC ₃ H ₇	H	H	4-OH-C ₆ H ₄	44	48	1.1	nd	nd
26	nC ₃ H ₇	nC ₃ H ₇	OH	H	4-OH-C ₆ H ₄	115	102	0.89	nd	nd
27	nC ₃ H ₇	nC ₃ H ₇	H	OH	4-OH-C ₆ H ₄	11	118	10.7	nd	nd
28	nC ₃ H ₇	nC ₃ H ₇	H	H	4-CH ₃ O-C ₆ H ₄	490	199	0.41	nd	nd
29	nC ₃ H ₇	nC ₃ H ₇	OH	H	4-CH ₃ O-C ₆ H ₄	479	631	1.3	nd	nd
30	nC ₃ H ₇	nC ₃ H ₇	H	OH	4-CH ₃ O-C ₆ H ₄	24	148	6.2	nd	nd
31	nC ₃ H ₇	nC ₃ H ₇	H	OH	4-CH ₃ CO-C ₆ H ₄	71	324	4.6	nd	nd
32	nC ₃ H ₇	nC ₃ H ₇	H	OH	4-NO ₂ -C ₆ H ₄	50	145	2.9	nd	nd
33	nC ₃ H ₇	nC ₃ H ₇	H	OH	4-CH ₃ SO ₂ -C ₆ H ₄	6.5	28	4.3	63	295
34	nC ₃ H ₇	CH ₃	H	OH	4-CH ₃ SO ₂ -C ₆ H ₄	64	468	7.3	240	7%
35	nC ₃ H ₇	nC ₃ H ₇	H	OH	2-Furyl	23	104	4.5	nd	nd
36	nC ₃ H ₇	nC ₃ H ₇	H	OH	4-COOH-C ₆ H ₄	338	933	2.8	nd	nd
37	nC ₃ H ₇	nC ₃ H ₇	H	OSO ₃ H	2-Furyl	35	408	11.7	nd	nd

^a Affinity values at the indicated human cloned ARs are expressed as K_i (nM) or as % of inhibition at a 1 μM concentration. SEMs were always lower than 10%.

^b SI is the selectivity index defined as the ratio K_i hA_{2A}/K_i hA_{2B}.

^c nd stands for not determined.

To improve water solubility of 8-(2-furyl)-9-OH-9-dAX derivative **35**, its sulfuric ester **37** was prepared by an esterification reaction with chlorosulfonic acid in pyridine.⁴³

Finally, 8-*p*-oxyacetamido-9-OH-9-dAX derivatives **38** and **40** were prepared from the corresponding *p*-oxyacetic ester **42** by a reaction with *p*-bromoaniline and 4-*N*-benzyl-piperazine, respectively, using NaCN as catalyst, as indicated in Scheme 4.³⁵

3. Molecular modeling

To evaluate the main differences between some molecular properties of 9-dAXs and 9-OH-9-dAXs a computational study was carried out on reference molecules **A** and **B** (Chart 2).

For the same purpose, water solubilities, and HPLC capacity factors as experimental descriptors of lipophilicity, were measured for selected 9-dAX and 9-OH-9-dAX derivatives (see Table 3).

The calculation of the MEP around position 9 returned for molecule **B** lower MEP values than the bound threshold equal to 1.06 kcal/mol observed for 9-dAX **A**. Along with MEPs, other relevant molecular interaction fields (MIFs) were calculated within GRID.⁴⁴ Unlike other traditional approaches, GRID has the advantage of considering the entire system immersed in water with a bulk dielectric constant ranging from 80, in the aqueous environment surrounding the target, to 4, in the deep center of globular macromolecular targets; this allows GRID to more realistically feature biological interactions. In this regard, the occurrence of putative HB interactions of reference molecules **A** and **B** was eval-

uated by using the H₂O probe which easily detected the emergence of HB interactions. As expected, the presence of the 9-hydroxyl group was relevant to engage HB interaction as indicated by the cyan mesh, contoured at a value of −4.0 kcal/mol, and surrounding position 9 only in the case of 9-OH-9-dAX reference molecule **B**.

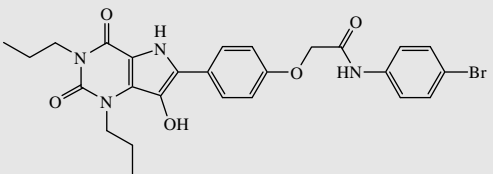
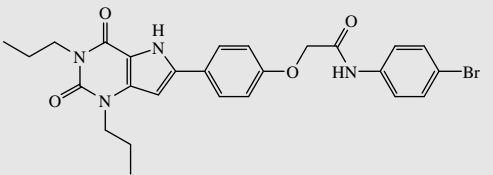
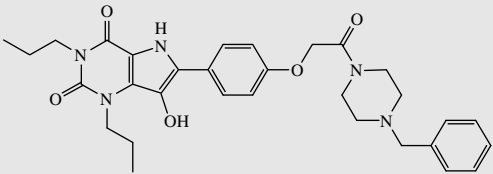
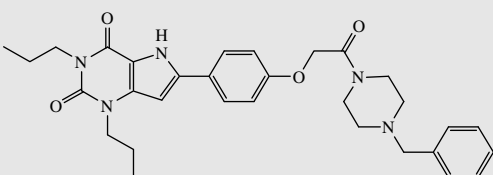
The difference in hydrophobic properties between molecules **A** and **B** may be well appreciated from MIF calculations with the DRY hydrophobic probe (data not shown). Taken together, these computational data do suggest for 9-OH-9-dAXs higher HB-making propensities, hydrophilicity and most likely, water solubility than 9-unsubstituted-9-dAXs (Fig. 2).

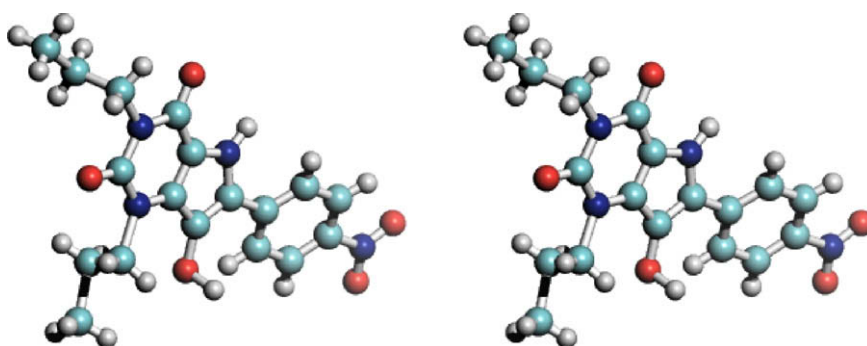
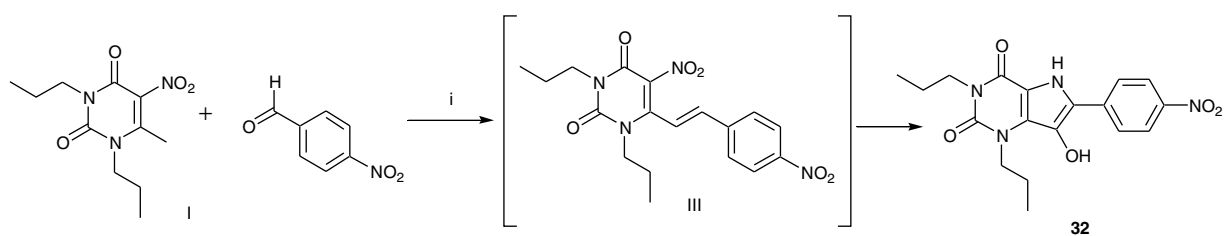
4. Biochemical and pharmacological assays

Compounds were assayed for their ability to displace [³H]-DPCPX, [³H]-ZM241385, [³H]-DPCPX and [³H]-NECA from cloned human A₁, A_{2A}, A_{2B} and A₃ ARs as described in our previous papers.^{35–37} All the active compounds showed competition concentration–response curves of specific radioligand binding against increasing concentrations of ligands, the slopes not being significantly different from unity at the 5% level of statistical significance (Fig. 3).

Antagonistic activity was measured for **38** by means of isolated organs assays at both rat colon A_{2B} and rat aorta A_{2A} AR subtypes. This compound concentration-dependently displaced the curves of the AR agonist NECA to the right in a parallel way without depres-

Table 2Chemical structures and *h*AR binding affinities^a of 1,3-dipropyl-8-*p*-oxyacetamido-9-dAX derivatives **38–41**

Compound	Chemical structure	K_i <i>hA</i> _{2B}	K_i <i>hA</i> _{2A}	SI ^b	K_i <i>hA</i> ₁	K_i <i>hA</i> ₃
38^c		1.0	100	100	79	1290
39		2.2	31	14	21	199
40		2.6	92	35	224	891
41		6.2	257	42	43	5%

^a Affinity values at the indicated human cloned ARs are expressed as K_i (nM) or as % of inhibition at a 1 μ mol concentration. SEMs were always lower than 10%.^b SI is the selectivity index defined as the ratio K_i *hA*_{2A}/ K_i *hA*_{2B}.^c In functional assays, compound **38** exhibited the following antagonist potency: pA_{2B} (rat) = 9.33 ± 0.28 , pA_{2A} (rat) = 6.65 ± 0.30 .**Figure 1.** Stereo-view of the X-ray crystallographic structure of **32**.**Scheme 2.** Reagents and conditions: (i) Piperidine, EtOH reflux.

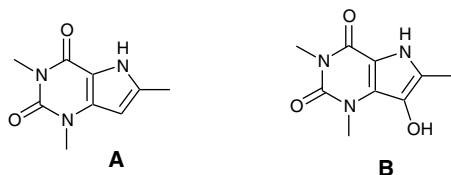
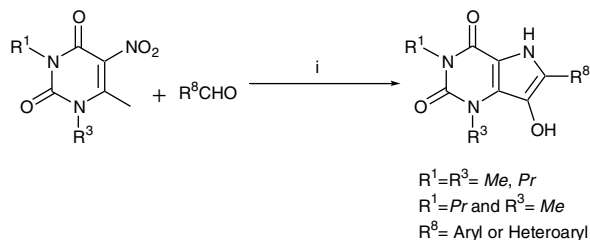


Chart 2. 9-dAX and 9-OH-9-dAX reference molecules.



11, 14, 15, 18, 21, 30–36, 42

Scheme 3. Reagents and conditions: (i) Piperidine, DMF, 400 W, 200 °C, 15 min.

sion of their maximum, compatible with a competitive antagonism (Fig. 4).

5. Results and discussion

Chemical structures of the examined ligands are reported in Tables 1 and 2 along with their binding affinities at the indicated AR subtypes. It must be kept in mind that the main goal of our research was the discovery of new and highly potent hA_{2B} antagonists endowed with good selectivity over hA_{2A} , measured by the selectivity index (SI), which is the ratio $K_i hA_{2A}/K_i hA_{2B}$. Accordingly, binding affinities at both the hA_{2B} and hA_{2A} ARs were first measured and only when good hA_{2B} AR affinity and SI were found, the affinities at hA_1 and hA_3 ARs were determined.

In addition, binding affinities at all four ARs were measured also for lead compounds **16** and **18** for a more sound evaluation of the SSRs. In Table 1, only the percentage of radioligand displacement at 1 μ M was reported for low-active compounds or for the ones whose low solubility in the assay medium prevented the determination of their K_i .

After structural assignment, 1,3-dipropyl-8-*p*-nitrophenyl-9-OH-9-dAX **32** was assayed at both hA_{2B} and hA_{2A} ARs. A good affinity at hA_{2B} ($K_i = 50$ nM) and a lower affinity at hA_{2A} ARs, resulting in a SI equal to 2.9, were measured. Bearing in mind the SARs and SSRs previously developed for a large series of 9-dAXs,^{35–37} a number of 1,3-dialkyl-8-(hetero)aryl-9- and -7-OH-9-dAXs were synthesized and tested together with their corresponding 7,9-unsubstituted-9-dAX analogues. 8-Aryl-1,3-dimethyl-9-dAXs **9–14** were envisaged as our initial target compounds.

1,3-Dimethyl-9-OH-9-dAXs **11** and **14** elicited sub-micromolar affinities at hA_{2B} and a low selectivity over hA_{2A} (SI = 5.1 and 4.8,

Table 3
Experimental and estimated physicochemical properties of selected 9-dAXs

Compound	$\log k_{60}^a$	$\log p^b$	$\log P^c$	Measured solubility ^d (μ g/ml)	Estimated solubility ^e (μ g/ml)
19	0.97	4.07	4.47	6 ± 2	10
21	0.83	3.04	3.88	30 ± 8	97
22	1.21	4.53	4.97	6 ± 2	5.4
24	0.96	3.50	4.38	30 ± 8	55
28	0.71	3.30	3.80	28 ± 5	38
30	0.51	2.26	3.21	120 ± 10	290
40	0.29	2.54	3.50	10 ± 2	9
41	0.93	3.79	3.14	2 ± 0.7	1.8

^a Isocratic RP-HPLC capacity factors determined on a C8 column, by using 60/40 methanol/water mixture as the mobile phase.⁴⁵

^b Computed by using ACD/Labs software (v. 11.00).⁴⁶

^c Computed by using Biolum software (v.1.5).⁴⁷

^d Measured solubility in a 50-mM Tris/HCl, pH 7.4 buffer by a turbidimetric method.⁴⁸

^e Computed by using ACD/Labs software (v. 11.00).⁴⁶

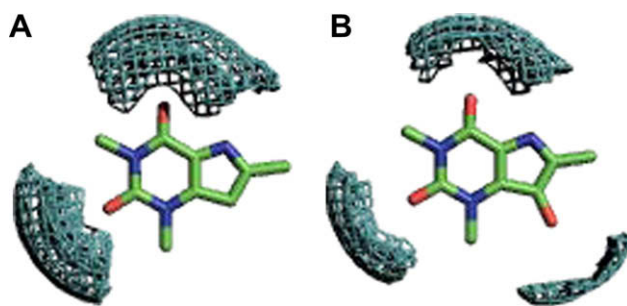


Figure 2. GRID MIF contoured at -4.0 kcal/mol using the H_2O probe for reference molecules **A** and **B**.

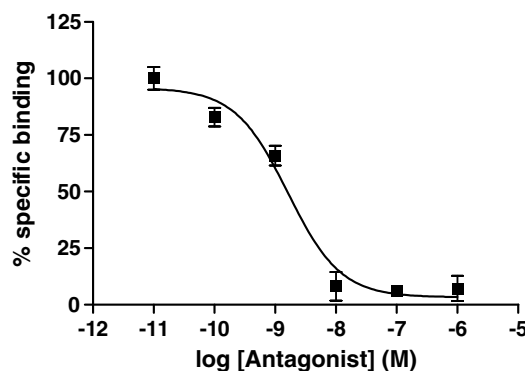
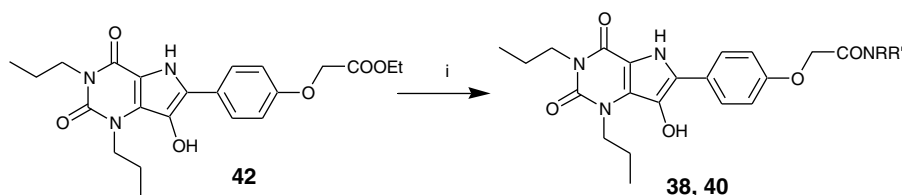


Figure 3. Binding competition experiments at cloned hA_{2B} receptors. Concentration–response curve for compound **38**. Values represent the mean \pm SEM (vertical bars) of two independent experiments.

respectively). The corresponding isomeric 7-OH-9-dAXs **10** and **13** exhibited even higher K_i s at hA_{2B} , whereas their low water solubility and affinity prevented the determination of K_i at the hA_{2A}



Scheme 4. Reagents and conditions: (i) $RR'NH$, NaCN, Δ .

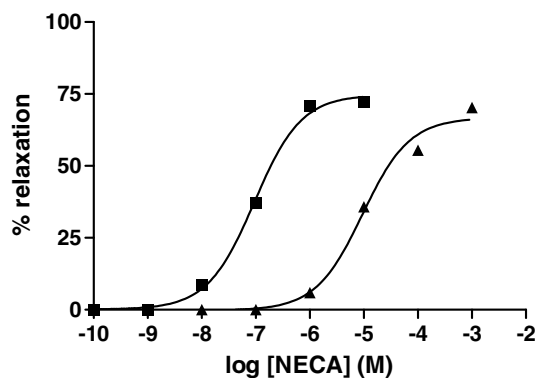


Figure 4. Isolated organ assays at rat A_{2B} receptors. Cumulative concentration-response curves to NECA in the absence (■) and in the presence (▲) of 30 nM **38**. The assay was performed in duplicate.

AR. The 7,9-unsubstituted 9-dAXs **9** and **12** exhibited a slightly improved hA_{2B} affinity compared to the corresponding 9-OH-9-dAXs **11** and **14** and SI values equal to 2.6 and 0.28, respectively. The latter value was quite surprising and unusual, since in our previous studies^{35–37} similarly substituted 9-dAXs always showed marked hA_{2B} selectivity.

These preliminary and somewhat discouraging results suggested us to introduce an electron-withdrawing group at the *para* position of the 8-phenyl ring since a similar substitution gave a good hA_{2B} affinity for 1,3-dipropyl-8-*p*-nitrophenyl-9-OH-9-dAX **32**. Very satisfactorily, *p*-methanesulfonylphenyl derivative **15** resulted as the most potent (K_i = 68 nM) and hA_{2B} -selective (SI = 10.2) ligand among the first series of targeted 1,3-dimethyl-9-dAX derivatives.

Guided by these initial findings, a new series of 1,3-dipropyl-8-(hetero)aryl-9-dAXs was designed, synthesized and tested aiming at an enhancement of hA_{2B} affinity, hA_{2B}/hA_{2A} selectivity and molecular hydrophilic properties. To this end, besides compounds **16–21** that are designed to make a direct affinity comparison with corresponding 1,3-dialkyl congeners **9–15**, new ligands bearing hydrophilic electron-withdrawing and electron-donor substituents in *para* position of the 8-phenyl ring were conceived.

With the only exception of compound **16**, 1,3-dipropyl derivatives **17–21** exhibited a hA_{2B} affinity higher than the corresponding 1,3-dimethyl analogues. However, the SI remained quite low, reaching a maximum equal to 3.2 for 9-dAX **19**. Comparing the hA_{2B} affinities of the three different classes of 1,3-dipropyl-9-dAXs, equally substituted at position 8, elicited the following hA_{2B} affinity ranking: 9-OH- > 7,9-unsubstituted- > 7-OH-9-dAXs.

Irrespective of the electron-withdrawing or electron-donor properties of the *para*-substituents of the 8-phenyl ring, several 1,3-dipropyl-9-OH-dAX derivatives showed, indeed, very high hA_{2B} affinities reaching low nanomolar K_i s with the *p*-OH (**27**) and *p*-SO₂CH₃ (**33**) congeners (K_i = 11 and 6.5 nM, respectively). It is worth noting that most *para*-substituents were strongly hydrophilic. This fact might thus increase water solubility and lower the partition coefficient allowing to overcome the most important pharmacokinetic drawbacks encountered in the vast series of 9-dAXs prepared recently by us.^{25,35–37} To support this hypothesis, water solubility and partition coefficient (*P*) of a selected number of 9-OH- and 7,9-unsubstituted-9-dAXs (see Table 3) were estimated by trustable software and experimentally measured by a turbidimetric assay in DMSO/buffer (pH = 7.4) and reverse-phase HPLC, respectively.

ACD (v. 11.00)⁴⁶ and Biolum (v. 1.5)⁴⁷ predicted quite different log *P*s but, as expected, both software programs indicated lower log *P*s for the 9-OH-9-dAXs (nearly 1 and 0.60 logarithmic unit dif-

ferences, respectively). This trend was experimentally confirmed by comparing the isocratic RP HPLC capacity factors (*k*) measured on a C8 column using a 60/40 methanol/water mixture as the mobile phase. With few exceptions, estimated and measured water solubility was relatively close, and indeed, a 5- to 10-fold increase was observed moving from 7,9-unsubstituted to 9-OH-9-dAXs. These encouraging findings prompted us to prepare two more hydrophilic 9-OH-9-dAXs, that is, 2-furyl derivative **35** and *p*-COOH-phenyl derivative **36**. While in the former a significant improvement of hA_{2B} affinity with respect to isosteric 8-phenyl derivative **18** was observed, the introduction of the ionized *p*-COOH group in the 8-phenyl ring of **18** led to a drop in affinity. Conversely, highly water-soluble hydrogen sulfate **37** maintained a good hA_{2B} affinity, comparable to that of its furyl precursor **35**, and even exhibited increased hA_{2B} selectivity (SI = 11.7 from 4.5).

Given that previous data^{35,36} have indicated an increased SI of 9-dAXs with ligands bearing larger alkyl substituents at position 1 than at position 3, we tried to enhance the SI of the most active ligand **33** by preparing its 3-methyl-1-propyl analogue **34**. Unfortunately, only a small increase of the SI was observed (from 4.3 to 7.3), but to the detriment of hA_{2B} affinity (nearly a 10-fold decrease).

Even in the absence of ligands with a high SI, 1,3-dipropyl-9-dAX derivatives **16**, **17**, **18**, **33** and **34** were selected for the evaluation of their binding affinities at the hA_1 and hA_3 ARs. Surprisingly, the 7,9-unsubstituted lead compound **16** at the hA_1 and hA_3 ARs exhibited higher affinities (K_i = 34 and 96 nM, respectively) than at hA_{2B} (K_i = 229 nM), whereas in the corresponding 9-OH congener **18** the affinity at hA_{2B} (K_i = 54 nM) remained higher than at the hA_1 and hA_3 ARs (K_i = 83 and 182 nM, respectively). The 7-OH-9-dAX lead compound **17** exhibited an unexpectedly high affinity at hA_1 (K_i = 25 nM) whereas at hA_3 a value of K_i > 1000 nM might be anticipated. Non symmetrically substituted 1-propyl-3-methyl-9-OH-9-dAX **34** displayed K_i values of 240 and supposedly >1000 nM at the hA_1 and hA_3 ARs, respectively, versus a value of K_i equal to 64 nM observed at hA_{2B} . Finally, 1,3-dipropyl-9-OH-9-dAX derivative **33** turned out to be the only ligand with a significant, albeit small, selectivity for the hA_{2B} receptor subtype yielding K_i values of 6.5, 28, 63 and 295 nM at the hA_{2B} , hA_{2A} , hA_1 and hA_3 ARs, respectively.

Since the above findings did not fulfill our expectations, especially about selectivity, we synthesized two additional 1,3-dipropyl-9-OH-9-dAXs (**38** and **40**, Table 2) designed on the basis of the good hA_{2B} affinity and selectivity observed by us and Jacobson in *p*-oxyacetamido-9-deazaxanthine^{35,36} and xanthine³⁰ derivatives (e.g., **4–5** and **3**, respectively, Chart 1). The two novel ligands, **38** and **40**, displayed excellent affinity at the hA_{2B} AR subtype (K_i = 1.0 and 2.6 nM, respectively) and significantly higher selectivity than that observed for all the other ligands reported in Table 1. The SIs referred to the K_i ratios hA_{2A}/hA_{2B} , hA_1/hA_{2B} and hA_3/hA_{2B} were 100, 79 and 1290 and 35, 86 and 342 for compounds **38** and **40**, respectively. Both the affinity and selectivity data of 9-OH-9-dAXs were significantly improved compared with those measured for the corresponding 7,9-unsubstituted-9-dAXs **39** and **41** reported for comparison in Table 2. However, the water solubility of 9-OH-9-dAXs **40**, 5-fold higher than that observed for the corresponding 7,9-unsubstituted-9-dAXs **41**, remained quite low. The substitution of the highly lipophilic benzyl group with smaller and more hydrophilic alkyl substituents might allow to overcome this problem.

1,3-Dipropyl-9-OH-9-dAX **38**, the most potent and selective hA_{2B} AR ligand discovered in the present work was tested also for its antagonistic activity at the A_{2A} and A_{2B} AR subtypes in isolated organ assays in rat. The pA_2 values at both receptor subtypes are reported in Table 2 (footnote c) along with the corresponding K_i values from binding assays. Full antagonism was observed with

pA_2 values very close to the corresponding pK_i s for both AR subtypes: A_{2B} : 9.33 vs 9.00 and A_{2A} : 6.65 vs 7.00.

6. Conclusions

The synthesis and comparative analysis of the biological activity at the AR subtypes of a large array of 9-OH-9-dAX derivatives allowed us to identify the main structural features for both high hA_{2B} affinity and hA_{2B}/hA_{2A} selectivity for this new class of AR ligands. A number of 9-OH-9-dAX derivatives with good hA_{2B} affinity ($K_i < 50$ nM) were obtained, whereas only very few ligands with a value of SI > 10 were found. Among these, compound **38** was particularly interesting, both in terms of hA_{2B} affinity ($K_i = 1.0$ nM) and selectivity over hA_{2A} , hA_1 and hA_3 (SI = 100, 79 and 1290, respectively).

Interestingly, this highly potent and selective hA_{2B} ligand revealed outstanding antagonist activities in a functional assay on the A_{2B} AR subtype on rat, with a $pA_2 = 9.33$, a value closely comparable to the pK_i (9.00) measured in the binding affinity assay at the corresponding cloned hAR.

Finally, by preparing a series of hydrophilic 9-OH-9-dAXs with higher water solubility and lower partition coefficients than the corresponding 9-dAXs, we were able to potentially improve the bioavailability of our compounds.

Taken together, our results show that suitably functionalised 9-OH-9-dAXs represent a class of highly active and hA_{2B} -selective AR antagonists with promising potential as antiasthmatic agents.

7. Experimental

7.1. Chemistry

High analytical grade chemicals and solvents were from commercial suppliers. When necessary, solvents were dried by standard techniques and distilled. After extraction from aqueous layers, the organic solvents were dried over anhydrous magnesium or sodium sulfate. Microwave-assisted reactions were carried out on a Micro SYNTH (Milestone). Thin-layer chromatography (TLC) was performed on aluminum sheets precoated with silica gel 60 F254 (0.2 mm) type E. Merck. Chromatographic spots were visualized by UV light or Hanessian reagent.⁴⁹ Purification of crude compounds was carried out by flash column chromatography on silica gel 60 (Kieselgel 0.040–0.063 mm, E. Merck) or by crystallization. Melting points (uncorrected) for fully purified products (see below) were determined in a glass capillary tube on a Stuart Scientific electrothermal apparatus SMP3. ¹H NMR spectra were recorded at 300 MHz on a Varian Mercury 300 instrument. All the detected signals were in accordance with the proposed structures. Chemical shifts (δ scale) are reported in parts per million (ppm) relative to the central peak of the solvent. Coupling constant (J values) are given in hertz (Hz). Spin multiplicities are given as: s (singlet), bs (broad singlet), d (doublet), t (triplet), q (quadruplet) or m (multiplet). ESI-MS was performed with an Electrospray interface Ion Trap Mass spectrometer. (1100 series LC/MSD Trap System Agilent, Palo Alto, Ca). Elemental analyses were performed on a Eurovector 300 C, H, N analyzer. Fully purified products had satisfactory C, H, N analyses (within $\pm 0.4\%$ of theoretical values). Reaction yields, crystallization solvent, melting points and spectral data of all the newly synthesized compounds are reported in Table 4.

Compounds **9** and **22** have been already described in Ref. 37, whereas compounds **12**, **13**, **16**, **17**, **19**, **20**, **28** and **29** have been reported in Ref. 38. Compounds **39** and **41** have been described in Refs. 35 and 36, respectively.

8-Substituted-7-OH-9-dAXs **10** and **26**, and the novel 9-dAX **25**, were obtained from 1,3-dialkyl-5-nitro-6-styryl uracil by a reductive cyclization with $SnCl_2$ in DMF at room temperature or under reflux, respectively, according to our reported methods.³⁸

7.1.1. General procedure for the synthesis of 6-(hetero)aryl-7-OH-1H-pyrrolo[3,2-d]pyrimidine-2,4(3H,5H)-diones **11**, **14**, **15**, **18**, **21**, **30–36**, **42**

In a microwave reactor, charged with a magnetic stirring bar, 1 mmol of 1,3-dialkyl-5-nitro-6-methyl-uracil, 1 mmol of (*p*-substituted)-benzaldehyde, or 2-furylaldehyde, and piperidine (0.13 ml, 2.5 mmol) were dissolved in 3 ml of DMF. The reaction mixture was heated by microwave irradiation at 200 °C (5 min of ramping, 400 W maximum power) for 15 min. The mixture was cooled to room temperature and the solvent was evaporated to dryness under vacuum and the oily residue, treated with absolute EtOH, afforded a solid compound that was filtered and crystallized.

7.1.2. 6-(4-Amino-phenyl)-5-hydroxy-1,3-dipropyl-1H-pyrrolo[3,2-d]pyrimidine-2,4(3H,5H)-dione **23**

N-[4-(5-Hydroxy-2,4-dioxo-1,3-dipropyl-2,3,4,5-tetrahydro-1H-pyrrolo[3,2-d]pyrimidin-6-yl)-phenyl]-acetamide³⁸ (0.34 g, 0.9 mmol) was dissolved in 5 ml of a: EtOH/1N NaOH (1/1) mixture and refluxed for 2 h. After cooling the solution was acidified and the precipitate was collected by filtration and crystallized.

7.1.3. 6-(4-Amino-phenyl)-7-hydroxy-1,3-dipropyl-1H-pyrrolo[3,2-d]pyrimidine-2,4(3H,5H)-dione **24**

Compound **32** (0.15 g, 0.4 mmol) was dissolved in 5 ml of DMF. $SnCl_2$ dihydrate (0.9 g, 4 mmol) was added and the mixture was stirred at room temperature for 2 h, poured into cold water and washed with AcOEt. The organic layer was dried on Na_2SO_4 and evaporated under vacuum to give an oil that was purified by flash chromatography ($CHCl_3$ /MeOH, 8/2) and then crystallized.

7.1.4. 6-(4-Hydroxy-phenyl)-7-hydroxy-1,3-dipropyl-1H-pyrrolo[3,2-d]pyrimidine-2,4(3H,5H)-dione **27**

Compound **30** (0.12 g, 0.3 mmol) was dissolved in 2 ml of dry DCM and cooled at 0 °C. Two milliliters of a solution 1M BBr_3 in DCM were added and the reaction was stirred at 0 °C for 1 h. The reaction mixture was poured into water and the organic layer washed three times with water, dried on Na_2SO_4 and evaporated affording a solid compound that was crystallized.

7.1.5. 6-(2-Furyl)-2,4dioxo-1,3-dipropyl-2,3,4,5-tetrahydro-1H-pyrrolo[3,2-d]pyrimidin-7-yl hydrogen sulfate **37**

Compound **35** (0.044 g, 0.14 mmol) was dissolved in dry pyridine (1 mL) and cooled to 0 °C. To this solution was added chlorosulfonic acid (0.163 g, 1.4 mmol) and the mixture allowed to warm to room temperature overnight. Evaporation afforded a residue which was treated with 2N HCl giving a precipitate that was crystallized from water.

7.1.6. General procedure for the synthesis of 1,3-dipropyl-9-OH-8-(4-*N*-substituted-oxyacetamido-phenyl)-9-dAX **38** and **40**

The reaction took place in a sealed tube under argon atmosphere. A catalytic amount of sodium cyanide (1 mg, 0.02 mmol) was added to ester **42** (0.065 g, 0.15 mmol) (see Scheme 4) and 16 mmol of amines. In the case of benzyl piperazine the reaction mixture was heated at 150 °C, whereas for 4-Br-aniline 2 mL of anhydrous dioxane was used as solvent and the reaction heated at 100 °C. The reactions were monitored by TLC, and when no more starting material was observed, the mixture was cooled to room temperature and treated with ethyl ether. The precipitate was isolated by filtration, washed with ethyl ether and crystallized yielding title compounds **38** and **40**.

7.2. X-ray crystallography

Crystals of 1,3-dipropyl-8-*p*-nitrophenyl-9-OH-9-dAX derivative **32** were obtained from methanol by slow evaporation. X-ray

Table 4

Reaction yields, crystallization solvents, melting points and spectral data of the newly synthesized 9-dAX derivatives

Compound	Yield (%)	Mp (°C) (crystallization solvent)	¹ HNMR (DMSO- <i>d</i> ₆) ^a	(Molecular formula) ESI/MS (<i>m/z</i>)
10	98	224–226 (EtOH)	11.84 (s, 1H), 7.80–7.77 (m, 2H), 7.49–7.41 (m, 3H), 6.38 (s, 1H), 3.61 (s, 3H), 3.22 (s, 3H)	(C ₁₄ H ₁₃ N ₃ O ₂) 270 [M–H] [–]
11 (lit. 39, 40, 41)	55	>250 (EtOH)	11.79 (s, 1H), 8.32 (s, 1H), 7.95–7.92 (m, 2H), 7.43–7.40 (m, 2H), 7.28–7.25 (m, 1H), 3.60 (s, 3H), 3.21 (s, 3H)	(C ₁₄ H ₁₃ N ₃ O ₃) 270 [M–H] [–]
14 (lit. 39, 40, 41)	51	>250° (EtOH)	11.75 (s, 1H), 8.28 (s, 1H), 7.83 (d, <i>J</i> = 8.0 Hz, 2H), 7.21 (d, <i>J</i> = 8.0 Hz, 2H), 3.60 (s, 3H), 3.23 (s, 3H), 2.30 (s, 3H)	(C ₁₅ H ₁₅ N ₃ O ₃) 284 [M–H] [–]
15^b	73	>250 (EtOH)	8.45 (bs, 1H), 8.21 (d, <i>J</i> = 8.5 Hz, 2H), 7.88 (d, <i>J</i> = 8.5 Hz, 2H), 3.60 (s, 3H), 3.23 (s, 3H), 3.21 (s, 3H)	(C ₁₅ H ₁₅ N ₃ O ₅ S) 348 [M–H] [–]
18	56	218–220 (EtOH)	11.80 (s, 1H), 8.29 (s, 1H), 7.93–7.91 (m, 2H), 7.43–7.38 (m, 2H), 7.28–7.25 (m, 1H), 4.09 (t, <i>J</i> = 7.4 Hz, 2H), 3.84 (t, <i>J</i> = 7.4 Hz, 2H), 1.70–1.48 (m, 4H), 0.89–0.82 (m, 6H)	(C ₁₈ H ₂₁ N ₃ O ₃) 326 [M–H] [–]
21	58	192 dec. (EtOH)	11.74 (s, 1H), 8.24 (s, 1H), 7.82 (d, <i>J</i> = 8.2 Hz, 2H), 7.21 (d, <i>J</i> = 8.2 Hz, 2H), 4.08 (t, <i>J</i> = 7.1 Hz, 2H), 3.83 (t, <i>J</i> = 6.9 Hz, 2H), 2.30 (s, 3H), 1.72–1.47 (m, 4H), 0.88–0.81 (m, 6H)	(C ₁₉ H ₂₃ N ₃ O ₃) 340 [M–H] [–]
23	51	>250 (EtOH/Et ₂ O)	11.53 (s, 1H), 7.49 (d, <i>J</i> = 8.5 Hz, 2H), 6.59 (d, <i>J</i> = 8.5 Hz, 2H), 6.17 (s, 1H), 5.45 (bs, 2H), 3.85–3.80 (m, 4H), 1.65–1.50 (m, 4H), 0.90–0.82 (m, 6H)	(C ₁₈ H ₂₂ N ₄ O ₃) 341 [M–H] [–]
24	82	200–201 (EtOH/Et ₂ O)	11.42 (s, 1H), 7.97 (s, 1H), 7.61 (d, <i>J</i> = 8.5 Hz, 2H), 6.56 (d, <i>J</i> = 8.5 Hz, 2H), 5.29 (s br, 2H), 4.07 (m, 2H), 3.81 (m, 2H), 1.68–1.50 (m, 4H), 0.88–0.81 (m, 6H)	(C ₁₈ H ₂₂ N ₄ O ₃) 341 [M–H] [–]
25	98	>250 (EtOH)	12.09 (s, 1H), 9.72 (s, 1H), 7.71 (d, <i>J</i> = 8.4 Hz, 2H), 6.78 (d, <i>J</i> = 8.4 Hz, 2H), 6.54 (s, 1H), 3.83–3.81 (m, 4H), 1.67–1.51 (m, 4H), 0.91–0.82 (m, 6H)	(C ₁₈ H ₂₁ N ₃ O ₃) 326 [M–H] [–]
26	98	218 dec. (EtOH)	11.65 (s, 1H), 9.78 (s, 1H), 7.62 (d, <i>J</i> = 8.8 Hz, 2H), 6.83 (d, <i>J</i> = 8.8 Hz, 2H), 6.54 (s, 1H), 3.85–3.81 (m, 4H), 1.65–1.51 (m, 4H), 0.91–0.82 (m, 6H)	(C ₁₈ H ₂₁ N ₃ O ₄) 342 [M–H] [–]
27	76	137 dec. (EtOH)	11.58 (s, 1H), 9.60 (s, 1H), 8.09 (s, 1H), 7.74 (d, <i>J</i> = 8.5 Hz, 2H), 6.78 (d, <i>J</i> = 8.5 Hz, 2H), 4.08 (t, <i>J</i> = 7.2 Hz, 2H), 3.82 (t, <i>J</i> = 7.2 Hz, 2H), 1.65–1.52 (m, 4H), 0.87–0.81 (m, 6H)	(C ₁₈ H ₂₁ N ₃ O ₄) 342 [M–H] [–]
30	55	205 dec. (EtOH)	11.68 (s, 1H), 8.18 (s, 1H), 7.88 (d, <i>J</i> = 8.8 Hz, 2H), 6.98 (d, <i>J</i> = 8.8 Hz, 2H), 4.08 (t, <i>J</i> = 7.2 Hz, 2H), 3.83 (t, <i>J</i> = 7.2 Hz, 2H), 3.76 (s, 3H), 1.66 (q, <i>J</i> = 7.2 Hz, 2H), 1.54 (q, <i>J</i> = 7.2 Hz, 2H), 0.88–0.81 (m, 6H)	(C ₁₉ H ₂₃ N ₃ O ₄) 356 [M–H] [–]
31	63	183 dec. (EtOH)	11.99 (s, 1H), 8.56 (s, 1H), 8.10 (d, <i>J</i> = 8.0 Hz, 2H), 7.98 (d, <i>J</i> = 8.0 Hz, 2H), 4.10 (t, <i>J</i> = 6.3 Hz, 2H), 3.84 (t, <i>J</i> = 6.3 Hz, 2H), 2.57 (s, 3H), 1.70–1.51 (m, 4H), 0.90–0.82 (m, 6H)	(C ₂₀ H ₂₃ N ₃ O ₄) 368 [M–H] [–]
32	68	>250 (EtOH)	12.16 (s, 1H), 8.78 (s, 1H), 8.28–8.20 (m, 4H), 4.10 (t, <i>J</i> = 7.4 Hz, 2H), 3.85 (t, <i>J</i> = 7.3 Hz, 2H), 1.71–1.54 (m, 4H), 0.90–0.82 (m, 6H)	(C ₁₈ H ₂₀ N ₄ O ₅) 371 [M–H] [–]
33	59	>250 (EtOH)	12.07 (s, 1H), 8.64 (s, 1H), 8.19 (d, <i>J</i> = 8.5 Hz, 2H), 7.93 (d, <i>J</i> = 8.5 Hz, 2H), 4.10 (t, <i>J</i> = 7.2 Hz, 2H), 3.84 (t, <i>J</i> = 7.2 Hz, 2H), 3.22 (s, 3H), 1.71–1.51 (m, 4H), 0.89–0.82 (m, 6H)	(C ₁₉ H ₂₃ N ₃ O ₅ S) 404 [M–H] [–]
34	68	>250 (EtOH)	12.06 (s, 1H), 8.68 (s, 1H), 8.20 (d, <i>J</i> = 8.5 Hz, 2H), 7.94 (d, <i>J</i> = 8.5 Hz, 2H), 3.85 (t, <i>J</i> = 7.2 Hz, 2H), 3.61 (s, 3H), 3.21 (s, 3H), 1.60–1.54 (m, 2H), 0.86 (t, <i>J</i> = 7.3 Hz, 3H)	(C ₁₇ H ₁₉ N ₃ O ₅ S) 376 [M–H] [–]
35	49	>250 (EtOH)	11.89 (s, 1H), 8.37 (s, 1H), 7.74 (s, 1H), 6.89–6.88 (m, 1H), 6.60–6.58 (m, 1H), 4.07 (t, <i>J</i> = 7.2 Hz, 2H), 3.81 (t, <i>J</i> = 7.2 Hz, 2H), 1.69–1.41 (m, 4H), 0.90–0.81 (m, 6H)	(C ₁₆ H ₁₉ N ₃ O ₄) 316 [M–H] [–]
36^c	65	>250 (EtOH)	11.98 (s, 1H), 8.54 (s, 1H), 8.07 (d, <i>J</i> = 8.5 Hz, 2H), 7.93 (d, <i>J</i> = 8.5 Hz, 2H), 4.10 (t, <i>J</i> = 7.2 Hz, 2H), 3.84 (t, <i>J</i> = 7.2 Hz, 2H), 1.71–1.57 (m, 4H), 0.90–0.82 (m, 6H)	(C ₁₉ H ₂₁ N ₃ O ₅) 370 [M–H] [–]
37	42	>250 (H ₂ O)	11.89 (s, 1H), 8.88 (bs, 1H), 7.74 (s, 1H), 6.89–6.88 (m, 1H), 6.60–6.58 (m, 1H), 4.07 (t, <i>J</i> = 7.2 Hz, 2H), 3.81 (t, <i>J</i> = 7.2 Hz, 2H), 1.69–1.41 (m, 4H), 0.90–0.81 (m, 6H)	(C ₁₆ H ₁₉ N ₃ O ₇ S) 396 [M–H] [–]
38	35	172 dec. (H ₂ O/MeOH)	11.68 (s, 1H), 10.22 (s, 1H), 8.19 (s, 1H), 7.88 (d, <i>J</i> = 8.8 Hz, 2H), 7.61 (d, <i>J</i> = 8.0 Hz, 2H), 7.50 (d, <i>J</i> = 8.0 Hz, 2H), 7.04 (d, <i>J</i> = 8.8 Hz, 2H), 4.73 (s, 2H), 4.08 (m, 2H), 3.83 (m, 2H), 1.67–1.50 (m, 4H), 0.88–0.81 (m, 6H)	(C ₂₆ H ₂₇ BrN ₄ O ₅) 555 [M–H] [–]
40	38	177 dec. (H ₂ O/MeOH)	11.68 (s, 1H), 8.19 (s, 1H), 7.84 (d, <i>J</i> = 8.8 Hz, 2H), 7.31–7.26 (m, 5H), 6.95 (d, <i>J</i> = 8.8 Hz, 2H), 4.84 (s, 2H), 4.08 (t, <i>J</i> = 7.2 Hz, 2H), 3.83 (t, <i>J</i> = 7.2 Hz, 2H), 3.48 (s, 2H), 3.44–3.55 (m, 4H), 2.30–2.24 (m, 4H), 1.67–1.50 (m, 4H), 0.88–0.81 (m, 6H)	(C ₃₁ H ₃₇ N ₅ O ₅) 558 [M–H] [–]
42	46	183 dec. (EtOH)	11.69 (s, 1H), 8.19 (s, 1H), 7.86 (d, <i>J</i> = 8.8 Hz, 2H), 6.97 (d, <i>J</i> = 8.8 Hz, 2H), 4.80 (s, 2H), 4.15 (q, <i>J</i> = 7.1 Hz, 2H), 4.08 (t, <i>J</i> = 6.9 Hz, 2H), 3.83 (t, <i>J</i> = 7.0 Hz, 2H), 1.70–1.50 (m, 4H), 1.20 (t, <i>J</i> = 7.1 Hz, 3H), 0.91–0.81 (m, 6H)	(C ₂₂ H ₂₇ N ₃ O ₆) 428 [M–H] [–]

^a Heteronuclear protons were detected by exchange with D₂O.^b N₇H proton was undetectable.^c COOH proton was undetectable.

intensity data were collected on a Syntex P21 diffractometer equipped with graphite monochromatized Cu-K α radiation. The structure was solved by direct methods and refined anisotropically by using the program package SIR 2002.⁵⁰ Crystallographic data (excluding structure factors) have been deposited at the Cambridge Crystallographic Data Centre and allocated the deposition number CCDC 693408. Copies of the data can be obtained, free of charge, on application to CCDC, 12 Union Road, Cambridge CB2 1EZ, UK [fax: +44 (0)1223-336033 or e-mail: deposit@ccdc.cam.ac.uk].

7.3. Partition coefficients and water solubility

Log P values were estimated by using ACD/LogP⁴⁶ and Biolum software.⁴⁷

The RP-HPLC analyses were performed on a X-Terra[®] C8, 5 μ m 3.0 \times 150 mm, chromatographic column (Waters, Milford, MA,

USA) eluting with a mixture of water–methanol (40/60, v/v) as the mobile phase at a flow rate of 1.0 ml min^{–1}. A solution of KI in methanol was used for the determination of dead time (*t*₀). Retention times (*t*_r) were measured in minutes. Log*k*, calculated from the capacity factor (*k*) was taken as the lipophilicity index.

The protocol adopted for measuring aqueous solubility was as follows. The compound was dissolved in DMSO at a concentration of 1 μ g/ml (or 10 μ g/ml for the more soluble compounds). This solution was added in portion, (2 μ l at a time) to 1 ml of a 50 mM TRIS/HCl pH 7.4 buffer solution at room temperature. Typically a total of 14 additions were made so that the final volume of DMSO was well below 5%. The appearance of the precipitate was detected by an absorbance increase, due to light scattering by particulate material, in a dedicate diode array UV spectrometer (Agilent 8453). Increased UV absorbance was measured in the 600–800 nm range. In its simplest implementation, the precipitation

Table 5Experimental conditions used for radioligand binding assays on A₁, A_{2A}, A_{2B}, and A₃ h.ARs

	A ₁	A _{2A}	A _{2B}	A ₃
Buffer A	20 mM Hepes, 100 mM NaCl, 10 mM MgCl ₂ , 2 U/mL adenosine deaminase (pH = 7.4)	50 mM Tris–HCl, 1 mM EDTA, 10 mM MgCl ₂ , 2 U/mL adenosine deaminase (pH = 7.4)	50 mM Tris–HCl, 1 mM EDTA, 5 mM MgCl ₂ , 10 µg/mL bacitracine, 2 U/mL adenosine deaminase (pH = 6.5)	50 mM Tris–HCl, 1 mM EDTA, 5 mM MgCl ₂ , 2 U/mL adenosine deaminase (pH = 7.4)
Buffer B	20 mM Hepes, 100 mM NaCl, 10 mM MgCl ₂ , (pH = 7.4)	50 mM Tris–HCl, 1 mM EDTA, 10 mM MgCl ₂ (pH = 7.4)	50 mM Tris–HCl, 1 mM EDTA, 5 mM MgCl ₂ , (pH = 6.5)	50 mM Tris–HCl (pH = 7.4)
Plate	GF/C	GF/C	GF/B	GF/B
Radioligand	[³ H]DPCPX 2 nM	[³ H]ZM241385 3 nM	[³ H]DPCPX 25 nM	[³ H]NECA 30 nM
Non-specific binding	10 µM (R)-PIA	50 µM NECA	1000 µM NECA	100 µM (R)-PIA
Incubation	25 °C/60 min	25 °C/30 min	25 °C/30 min	25 °C/180 min

point (i.e., the upper aqueous solubility limit), was calculate from a bilinear curve fit in a plot of the absorbance (*y* axis) versus µl of DMSO (*x* axis).

7.4. Molecular modeling

Reference molecules **A** and **B** (Chart 2) were built from the SYBYL fragment libraries.⁵¹ Geometrical optimization and charge calculation were made by means of a quantum mechanical method with the PM3 Hamiltonian available in MOPAC 6.0.⁵² The molecular electrostatic potential (MEP) was calculated with VEGA-ZZ setting the point density and the probe radius equal to 1000 and 1.4 Å, respectively.⁵³ By using standard options, molecular interaction fields (MIFs) were calculated within GRID⁴⁴ using the H₂O and DRY probes.

7.5. Biochemistry and pharmacology

7.5.1. Radioligand binding assays

Radioligand binding competition assays were performed in vitro using A₁, A_{2A}, A_{2B} and A₃ human receptors expressed in transfected CHO (*hA₁*), HeLa (*hA_{2A}* and *hA₃*) and HEK-293 (*hA_{2B}*) cells. The experimental conditions used are summarized in Table 5. In each instance aliquots of membranes (15 µg for A₁, 10 µg for *hA_{2A}*, 18 µg for *hA_{2B}* and 100 µg for *hA₃*) in buffer A (see Table 5) were incubated for the specified time at 25 °C with the radioligand (2–35 nM) and six different concentrations (ranging from 0.1 nM to 10 µM) of the test molecule or standard in a final volume of 200 µl. The binding reaction was stopped by rapid filtration in a multiscreen manifold system (Milipore Iberica, Madrid, Spain). Unbound radioligand was removed by washing 4× with 250 µl ice-cold buffer B for *hA₁* and *hA_{2A}* receptors and 6× 250 µl ice-cold buffer B for *hA_{2B}* and *hA₃* receptors (see Table 5). Non specific binding was determined using a 50–1000 µM NECA solution for *hA_{2A}* and *hA_{2B}* receptors and 10–100 µM R-PIA solution for *hA₁* and *hA₃*. Radioactivity retained on filters was determined by liquid scintillation counting using Universol (ICN Biochemicals, Inc.). The binding affinities were determined using [³H]-DPCPX as the radioligand for A₁ and A_{2B}, [³H]-ZM241385 for A_{2A} and [³H]-NECA for A₃. The inhibition constant (*K_i*) of each compound was calculated by the Cheng–Prusoff expression $K_i = IC_{50}/(1 + (C/K_D))$ ⁵⁴ where *IC*₅₀ is the concentration of compound that displaces the binding of radioligand by 50%, *C* is the free concentration of radioligand and *K_D* is the apparent dissociation constant of the radioligand.

7.5.2. Isolated organ assays: A_{2A} receptors

These assays were performed in A_{2A} receptors⁵⁵ from isolated aorta of 200–250 g male Sprague–Dawley rats. The aorta was rapidly excised and placed in modified Krebs solution of the following composition (mM): NaCl 118; KCl 4.7; MgSO₄·7H₂O 1.2; CaCl₂·2H₂O 2.5; KH₂PO₄ 1.18; NaHCO₃ 25; glucose 11, and the

solution was maintained at 37 °C with aeration by carbogen (95% CO₂ + 5% O₂, pH 7.4 ± 0.1). The vessels were cleaned to remove connective tissue, cut into rings, 4 mm in length, and suspended between stainless steel wires in organ baths containing 20 mL of Krebs solution, under a basal tension of 2 g (maintained throughout the experiment). The aorta rings were stabilized for 60 min in the modified Krebs solution at 37 ± 0.2 °C continuously saturated with carbogen before the start of the assay, and during the stabilization time they were washed with new Krebs solution at least three times (15 min each time). All aorta rings were initially exposed to 0.1 µM phenylephrine to elicit a contractile response, and after this the presence of endothelium was confirmed by the addition of acetylcholine (10 µM). Tissues giving less than 25% relaxation of phenylephrine contraction were discarded. After a recovery time of 60 min with successive washes with fresh Krebs solution, a new phenylephrine contraction was elicited and responses to NECA were measured and used to construct cumulative relaxant–response curves. After a new recovery time of 60 min with successive washes with fresh Krebs solution. Antagonists were incubated for 30 min and then a new phenylephrine contraction was elicited and responses to NECA were measured and used to construct cumulative relaxant–response curves.

Isometric contractions were recorded by using Grass FTO3C force displacement transducers connected to a 7D Grass polygraph, signals were conducted through a UIM100 module (Biopac systems) to 16 digital channels to a MP100 data acquisition unit (Biopac systems).

Contractions were processed with Acknowledge 3.0 (Biopac) and analyzed with Kaleidagraph Software (Synergy Software). Data were finally represented by using GraphPad Prism 2.1 (GraphPad Software) by constructing sigmoidal curves representing the logarithm of the concentration of NECA vs maximal effect of the NECA in the presence and in the absence of the antagonist tested, obtaining values of EC₅₀ (concentration of NECA that exerts the 50% of maximal effect). Antagonistic potency of the compounds were calculated and expressed as pA₂ from this equation:

$$pA_2 = \log((EC_{50'}/EC_{50}) - 1)/C$$

where EC_{50'}/EC₅₀ is the ratio of concentrations of agonist giving an equal response (50% of the maximal effect) in the presence and in the absence, respectively, of a given concentration of the antagonist (*C*).⁵⁶

7.5.3. Isolated organ assays: A_{2B} receptors

Male Wistar–Kyoto rats (weighing 250–300 g) were sacrificed and distal colon was excised from them.⁵⁷ Colon was placed into Tyrode buffer (NaCl 136.9 mM; KCl 2.8 mM; MgSO₄·7H₂O 2.1; CaCl₂·2H₂O 1.8 mM; Na₂HPO₄ 0.3 mM; NaHCO₃ 11.9 mM; Glucose 5.6 mM) and dissected in sections of 10–15 mm in length. Sections were placed in an organ bath with Tyrode buffer at 37 °C and bub-

bled with carbogen (95% O₂, 5% CO₂) and attached to a force displacement transducer for registering isometric tension.

Sections were equilibrated at a basal tension of 1 g during 60 min, replacing the buffer each 15 min for fresh buffer.

Tissues were primed with 100 μ M bethanecol for three times, with a period of 60 min between each addition of bethanecol. After priming the tissues 100 μ M bethanecol was added and when the contraction was stable a cumulative concentration-response curve of NECA was performed (from 1 nM to 100 μ M). After that, tissues were washed four times for 15 min with fresh buffer (60 min of washing) and antagonists were added for 30 min. After this time, a new contraction of the tissue was performed with 100 μ M bethanecol and once the contraction was stable a new cumulative concentration-response curve of NECA was performed.

Isometric contractions were recorded and analyzed as for isolated organ assays at A_{2A} receptors.

Acknowledgments

The Italian authors thank the MIUR (Ministero dell'Istruzione, dell'Università e della Ricerca Scientifica), Rome (Italy), for financial support. The Spanish authors thank the Health Institute Carlos III (RD07/0067/0002) and Xunta de Galicia (07CSA003203PR) for partial financial support. J.M.B. is a recipient of a financial support from the Programa Isabel Barreto (Xunta de Galicia).

References and notes

- Jacobson, K. A.; Gao, Z.-G. *Nat. Rev. Drug. Discov.* **2006**, *5*, 247.
- Moro, S.; Gao, Z.-G.; Jacobson, K. A.; Spalluto, G. *Med. Res. Rev.* **2006**, *26*, 131.
- Akkari, R.; Burbiel, J. C.; Hockemeyer, J.; Müller, C. E. *Curr. Top. Med. Chem.* **2006**, *6*, 1375.
- Fredholm, B. B.; Ijzerman, A. P.; Jacobson, K. A.; Klotz, K. N.; Linden, J. *Pharmacol. Rev.* **2001**, *53*, 527.
- Volpini, R.; Costanzi, S.; Vittori, S.; Cristalli, G.; Klotz, K. N. *Curr. Top. Med. Chem.* **2003**, *3*, 427.
- Baraldi, P. G.; Romagnoli, R.; Preti, D.; Fruttarolo, F.; Carrion, M. D.; Tabrizi, M. A. *Curr. Med. Chem.* **2006**, *13*, 3467.
- Strohmeier, G. R.; Reppert, S. M.; Lencer, W. I.; Madara, J. L. *J. Biol. Chem.* **1995**, *270*, 2387.
- Papassotiropoulos, A.; Hock, C.; Nitsch, R. M. *Neurobiol. Aging* **2001**, *22*, 863.
- Harada, H.; Osamu Asano, O.; Hoshino, Y.; Yoshikawa, S.; Matsukura, M.; Kabasawa, Y.; Nijima, J.; Kotake, Y.; Watanabe, N.; Kawata, T.; Inoue, T.; Horizoe, T.; Yasuda, N.; Minami, H.; Nagata, K.; Murakami, M.; Nagaoka, J.; Kobayashi, S.; Tanaka, I.; Abe, S. *J. Med. Chem.* **2001**, *44*, 170.
- Linden, J. *Mol. Pharmacol.* **2005**, *1385*.
- Jacobson, K. A.; Hoffman, C.; Cattabeni, F.; Abbracchio, M. P. *Apoptosis* **1999**, *4*, 197.
- Xaus, J.; Valledor, A. F.; Cardo, M.; Marques, L.; Beleta, J.; Palacios, J. M.; Celada, A. *J. Immunol.* **1999**, *163*, 4140.
- Fozard, J. R.; McCarthy, C. *Curr. Opin. Invest. Drugs* **2002**, *3*, 69.
- Feoktistov, I.; Biaggioni, I. *J. Clin. Invest.* **1995**, *96*, 1979.
- Wolber, C.; Fozard, J. R. *Naunyn Schmiedeberg's Arch. Pharmacol.* **2005**, *371*, 158.
- Holgate, S. T. *Br. J. Pharmacol.* **2005**, *145*, 1009.
- Feoktistov, I.; Murray, J. J.; Biaggioni, I. *Mol. Pharmacol.* **1994**, *45*, 1160.
- Peyot, M.-L.; Gadeau, A.-P.; Dandré, F.; Belloc, I.; Dupuch, F.; Desgranges, C. *Circ. Res.* **2000**, *86*, 76.
- Feoktistov, I.; Biaggioni, I. *Drug. Dev. Res.* **1996**, *39*, 333.
- Jacobson, K. A.; Ukena, D.; Padgett, W.; Daly, J. W.; Kirk, K. L. *J. Med. Chem.* **1987**, *30*, 211.
- Müller, C. E.; Shi, D.; Manning, M.; Daly, J. W. *J. Med. Chem.* **1993**, *36*, 3341.
- Kim, S. A.; Marshall, M. A.; Melman, N.; Kim, H. S.; Müller, C. E.; Linden, J.; Jacobson, K. A. *J. Med. Chem.* **2002**, *45*, 2131.
- Grahner, B.; Winiwarter, S.; Lanzer, W.; Müller, C. E. *J. Med. Chem.* **1994**, *37*, 1526.
- Hayallah, A.; Sandoval-Ramirez, J.; Reith, U.; Schobert, U.; Preiss, B.; Schumacher, B.; Daly, J. W.; Müller, C. E. *J. Med. Chem.* **2002**, *45*, 1500.
- Vidal, B. J.; Esteve Trias, C.; Segarra Matamoros, V.; Ravina Rubira, E.; Fernandez Gonzales, F.; Loza Garcia, M. I.; Sanz Carreras, F.; WO Patent 03/000694, 2003.
- Kalla, R.; Perry, T.; Elzein, E.; Varkhedkar, V.; Li, X.; Ibrahim, P.; Palle, V.; Xiao, D.; Zablocki, J. US Patent 6825349, 2004.
- Palle, V.; Elzein, E.; Ibrahim, P.; Kalla, R.; Li, X.; Perry, T.; Varkhedkar, V.; Xiao, D.; Zablocki, J. WO Patent 05042534, 2005.
- Wang, G.; Rieger, J. M.; Thompson, R. D. WO patent 05021548, 2005.
- Kim, Y. C.; Ji, X.; Melman, N.; Linden, J.; Jacobson, K. A. *Drug. Dev. Res.* **1999**, *47*, 178.
- Kim, Y. C.; Ji, X.; Melman, N.; Linden, J.; Jacobson, K. A. *J. Med. Chem.* **2000**, *43*, 1165.
- Baraldi, P. G.; Tabrizi, M. A.; Preti, D.; Bovero, A.; Romagnoli, R.; Fruttarolo, F.; Abdel Zaid, N.; Moorman, A. R.; Varani, K.; Gessi, S.; Merighi, S.; Borea, P. A. *J. Med. Chem.* **2004**, *47*, 1434.
- Elzein, E.; Kalla, R.; Li, X.; Perry, T.; Gimbel, A.; Zeng, D.; Lustig, K.; Leung, K.; Zablocki, J. *J. Med. Chem.* **2008**, *51*, 2267.
- Vidal, B.; Esteve, C. WO Patent 03082873, 2003.
- Esteve, C.; Nueda, A.; Diaz, J. L.; Beleta, J.; Cardenas, A.; Lozoya, E.; Cadavid, M. I.; Loza, M. I.; Ryder, H.; Vidal, B. *Bioorg. Med. Chem. Lett.* **2006**, *51*, 3642.
- Carotti, A.; Cadavid, M. I.; Centeno, N. B.; Esteve, C.; Loza, M. I.; Martinez, A.; Nieto, R.; Ravina, E.; Sanz, F.; Segarra, V.; Sotelo, E.; Stefanachi, A.; Vidal, B. *J. Med. Chem.* **2006**, *49*, 282.
- Stefanachi, A.; Brea, J. M.; Cadavid, M. I.; Centeno, N. B.; Esteve, C.; Loza, M. I.; Martinez, A.; Nieto, R.; Ravina, E.; Sanz, F.; Segarra, V.; Sotelo, E.; Vidal, B.; Carotti, A. *Bioorg. Med. Chem.* **2008**, *16*, 2852.
- Carotti, A.; Stefanachi, A.; Ravina, E.; Sotelo, E.; Loza, M. I.; Cadavid, M. I.; Centeno, N. B.; Nicolotti, O. *Eur. J. Med. Chem.* **2004**, *39*, 879.
- Stefanachi, A.; Leonetti, F.; Cappa, A.; Carotti, A. *Tetrahedron Lett.* **2003**, *1121*.
- Senda, S.; Hirota, K.; Suzuki, M.; Takahashi, M. *Chem. Pharm. Bull.* **1977**, *25*, 568.
- Yoneda, F.; Motokura, M.; Otagiri, M. *Chem. Lett.* **1981**, *9*, 1273.
- Yoneda, F.; Motokura, M.; Kamishimoto, M.; Nagamatsu, T.; Otagiri, M.; Ukeama, K.; Takamoto, M. *Chem. Pharm. Bull.* **1982**, *9*, 3187.
- Smits, G.; Jin, X.; Gross, G.; Auchampach, J.; WO Patent 2003105666, 2003.
- Fairley, B.; Botting, N. P.; Cassidy, A. *Tetrahedron* **2003**, *59*, 5407.
- Goodford, P. J. *J. Med. Chem.* **1985**, *28*, 849.
- Kaliszan, R.; Nasal, A.; Markuszewski, M. *J. Anal. Bioanal. Chem.* **2003**, *377*, 803.
- Advanced Chemistry Development, Toronto, Canada.
- BioByte Corp., Claremont, CA, USA.
- Lipinski, C. A.; Lombardo, F.; Dominy, B. W.; Feeney, P. J. *Adv. Drug Deliv. Rev.* **2001**, *46*, 3.
- Touchstone, J. *Advances in Thin-layer Chromatography*; John Wiley & Sons: New York, 1982.
- Burla, M. C.; Carmalli, M.; Carrozzini, B.; Cascarano, G. L.; Giacobuzzo, C.; Palidori, G.; Spagna, R. *J. Appl. Crystallogr.* **2003**, *36*, 1103.
- SYBYL, version 7.1; Tripos Inc. (1699 South Hanley Road, St. Louis, MO 63144).
- Stewart, J. J. P. *Quant. Chem. Prog. Exch.* **1990**, *10*, 86.
- Pedretti, A.; Villa, L.; Vistoli, G. *J. Mol. Graphics* **2002**, *21*, 47.
- Cheng, Y.; Prusoff, W. H. *Biochem. Pharmacol.* **1973**, *22*, 3099.
- Prentice, D. J.; Hourani, S. M. O. *Br. J. Pharmacol.* **1996**, *118*, 1509.
- Furchgott, R. F. In *Catecholamines*; Blaschko, H., Muscholl, E., Eds.; Springer-Verlag: Heidelberg, 1972.
- Fozard, J. R.; Baur, F.; Wolber, C. *Eur. J. Pharmacol.* **2003**, *475*, 79.